International Journal of Mass Spectrometry 282 (2009) 85–90

Contents lists available at ScienceDirect

International Journal of Mass Spectrometry

journal homepage: www.elsevier.com/locate/ijms

Flowing afterglow studies of the electron recombination of protonated cyanides $(RCN)H^+$ and their proton-bound dimer ions $(RCN)_2H^+$ where R is H, CH_3, and CH_3CH_2

J.L. McLain, C.D. Molek, D. Osborne Jr., N.G. Adams*

University of Georgia, Athens, GA 30602, United States

ARTICLE INFO

Article history:
Received 22 November 2008
Received in revised form 5 February 2009
Accepted 6 February 2009
Available online 14 February 2009

Keywords:
Dissociative recombination
Electron–ion recombination
VT-FALP

ABSTRACT

A study has been made of the electron–ion dissociative recombination of the protonated cyanides ($RCNH^+$, R = H, CH_3, C_2H_5) and their proton-bound dimers $(RCN)_2H^+$ at 300 K. This has been accomplished with the flowing afterglow technique using an electrostatic Langmuir probe to determine the electron density decay along the flow tube. For the protonated species, the recombination coefficients, $\alpha_e(cm^3\ s^{-1})$, are $(3.6 \pm 0.5) \times 10^{-7}$, $(3.4 \pm 0.5) \times 10^{-7}$, $(4.6 \pm 0.7) \times 10^{-7}$ for R = H, CH_3, C_2H_5, respectively. For the proton-bound dimers, the α_e are substantially greater being $(2.4 \pm 0.4) \times 10^{-6}$, $(2.8 \pm 0.4) \times 10^{-6}$, $(2.3 \pm 0.3) \times 10^{-6}$ for R = H, CH_3, C_2H_5, respectively. Fitting of the electron density decay data to a simple model has shown that the rate coefficients for the three-body association of $RCNH^+$ with RCN are very large being $(2.0 \pm 0.5) \times 10^{-26}\ cm^6\ s^{-1}$. The significance of these data to the Titan ionosphere is discussed.

Published by Elsevier B.V.

1. Introduction

In Titan's atmosphere and the interstellar medium (ISM), cyanides are extremely important due to their large abundances. The interest in this topic is evident from the abundance of literature on RCN and $(RCN)H^+$ (R = H, CH_3). [1–9] $HCNH^+$ was predicted [1–4] to be a dominate ion in Titan's atmosphere and this was confirmed by the Cassini ion and neutral mass spectrometer (INMS) [5]. Its number density has approached 1000 cm^{-3}, a value almost 10 times that of any other ions in the altitude range ~1000–1300 km [5]. $HCNH^+$ also has been detected in the ISM along with vibrationally excited HCN [6,7]. In addition, CH_3CNH^+ is also an important ion in models of Titan's ionosphere contributing significantly to the total positive ionization density in the troposphere [10]. Microwave observations have detected CH_3CN in TMC-1 and Sgr B2 [8], and pure rotational transitions also were measured for CH_3CNH^+ in the range of 325–500 GHz in 2006 [9]. This and the next ion in this series, $CH_3CH_2CNH^+$, have also been included in models of Titan's atmosphere, but few kinetic studies have been performed [11–13]. These ions contribute significantly to ionization loss in these regions through the process of dissociative electron–ion recombination, DR. Because of this, and because DR is rapid, the present study was performed to determine DR rate coefficients (α_e) of these ions for use in chemical modeling applications. In addition, determination of α_e for a series of ions shows trends which provide information on reaction mechanisms. For these studies, a VT-FALP (variable temperature, flowing afterglow Langmuir probe) apparatus has been used. During these studies, it became evident that proton-bound dimers were rapidly produced. The study of DR of $RCNH^+$, where R = H, CH_3, C_2H_5, with electrons is straightforward since the reactions with the H_3^+ precursor give only non-dissociative proton transfer, and thus they can be generated as the only ion in the plasma [14–16]. On addition of RCN, these ions begin to recombine with electrons immediately and the reciprocal electron density changes with the flow tube position were very linear indicating that only one ion species is recombining in the plasma. Although this linearity is observed at all concentrations of RCN, the rate of electron density decay increased significantly in all cases with increasing concentration of RCN. It became apparent that this increase in the rate of electron decay is a result of the three-body association of $RCNH^+$ with RCN to form proton-bound dimer ions followed by their recombination. These types of dimer ions have been shown to have exceptionally large recombination rate coefficients. [17–19] As has also been predicted by theory [17], these associations are also rapid due to the large dipole moments of the cyanides. Since the electron density profile is now not of a single ionic species recombining but a mixture of two ionic species recombining simultaneously, numerical solution of the kinetic rate equations is necessary to obtain an accurate fit to all of the data [20]. This paper is concerned with the

* Corresponding author. Tel.: +1 706 542 3722; fax: +1 706 542 9454.
E-mail address: adams@chem.uga.edu (N.G. Adams).

1387-3806/$ – see front matter. Published by Elsevier B.V.
doi:10.1016/j.ijms.2009.02.004

determination of α_e for these protonated and proton-bound dimer cyanides.

2. Experiment

A variable temperature flowing afterglow technique with Langmuir probe diagnostics, VT-FALP, was used for these DR measurements. This technique has been described in detail in the literature and will only be discussed briefly here [21,22]. A He^+/He_2^+ plasma flow (also with helium metastables, He^m) was produced by a microwave discharge in helium flowing with a throughput of 16 slm along a flow tube (1 m long and 7 cm in diameter) at a pressure of ~1.5 Torr. Under these conditions He^+ rapidly associates with He generating He_2^+. Argon was added upstream in the flow at a concentration of $\sim 5 \times 10^{13}$ cm^{-3} to destroy all He^m and He_2^+ producing a predominantly Ar^+/e^- plasma. Hydrogen was then added further downstream to form an H_3^+/electron plasma by a standard reaction sequence [23]. These ions were sampled through an orifice to a downstream quadrupole mass filter/ion counting detection system which was used to identify all ions present in the plasma. RCN was then added to produce the recombining ions by proton transfer from H_3^+. Kinetic models were produced to confirm the ion chemistry occurring prior to the addition of RCN and have been presented in the literature [23]. The HCN gas was synthesized from the reaction H_2SO_4 + NaCN using a standard procedure [24]. The 99.9% acetonitrile (CH_3CN) was obtained from Aldrich® and 99% propanenitrile (CH_3CH_2CN) from Alfa Aesar®. Their neat vapors were often used to create the ions of interest after a series of freeze/pump/thaw procedures to remove any dissolved impurity gases. Dilutions with helium were used to obtain accurate values of the lower concentrations. The recombining ion types were created by the reactions:

$$H_3^+ + RCN \rightarrow [RCNH^+]^* + H_2 \qquad k_1 \tag{1}$$

$$[RCNH^+]^* + RCN \rightarrow RCN^* + RCNH^+ \qquad k_2 \tag{2}$$

where * indicates rovibronic internal excitation. At this point, only protonated-RCN ions were observed in the plasma. Eq. (1) has been shown at room temperature to be simply a proton transfer reaction for all of the cyanides studied here and all these proton transfers have rate coefficients approaching $\sim 1 \times 10^{-8}$ cm^3 s^{-1} [14–16]. Resonant proton transfer, Eq. (2), rapidly quenches any rovibronically excited species created by the exothermicity of the primary proton transfer reaction before recombination occurs. At the higher RCN concentrations, the association, Eq. (3), can become more rapid than DR of the protonated ions and are stabilized by a helium third body to create the proton-bound dimer. The resonant ligand switching reaction, Eq. (4), can then de-excite these dimers before recombination can occur.

$$RCNH^+ + RCN + He \rightarrow [(RCN)_2H^+]^* + He \qquad k_3 \tag{3}$$

$$[(RCN)_2H^+]^* + RCN \rightarrow (RCN)_2H^+ + RCN^* \qquad k_4 \tag{4}$$

A movable Langmuir probe (25 μm in diameter and 4.3 mm long) operating in the orbital limited regime, was used to determine the electron density [e^-] at various positions along the flow tube [25]. [e^-] and [e^-]$^{-1}$ are plotted as a function of time in Fig. 1, and the α_e's are determined by numerical solution of the rate equations. For a single ion species and when ambipolar diffusion losses are not included, the simple form of the rate equation is $1/[e^-]_t - 1/[e^-]_0 = \alpha_e t$. Although, ambipolar diffusion is small in our experiment, this effect was included in the kinetic models. At the highest RCN concentrations, approaching 1×10^{14} cm^{-3}, the Langmuir probe had to be cleaned considerably longer than normal due to surface contaminations of the probe by the cyanide vapors. Usually, after every voltage sweep, a negative voltage of 130 V was applied for ~5 s to heat the probe so as to obtain a clean surface and this resulted in exceptionally linear probe characteristics.

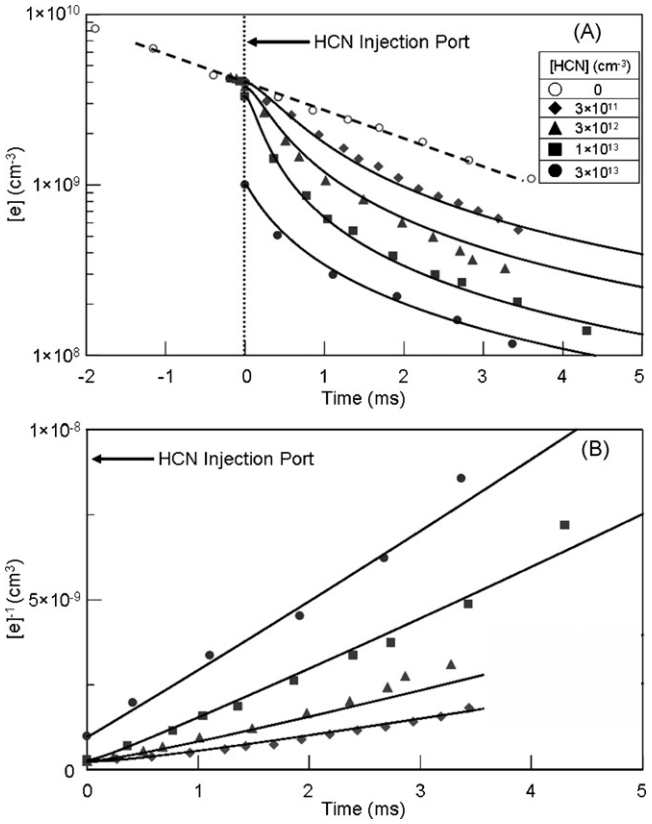

Fig. 1. Plot A illustrates electron density decays with time, and the kinetic model fit to the experimental data at a series of [HCN] concentrations. The open circles are with no HCN added to the flow and therefore the electron density decay is only due to diffusion and recombination of H_3^+, $\alpha_e = 1.1 \times 10^{-7}$ cm^3 s^{-1} under these conditions. Time zero represents the position in the flow tube at which HCN was added. Plot B shows a typical set of plots of 1/[e] vs. time for determining the α_e. The solid lines are the fits of the model to the experimental data to show the validity of the model even when two ionic species are recombining simultaneously. The upcurving of the data in B at late times is due to the increasing importance of diffusion.

3. Results and discussion

The form of the electron density profiles depended significantly on the RCN concentration which was varied from 1×10^9 to approaching 1×10^{14} cm^{-3}. This is because of the association of $RCNH^+$ with RCN to produce the $(RCN)_2H^+$, Eq. (3). To model the recombination, it was necessary to fit the data by numerically solving the kinetic equations for the production and recombination of the ions present in the afterglow. From this, the individual rates coefficients (k_3 and k_{-3}) for association and dissociation and the α_e's were obtained. To be valid, the models have to fit all of the data obtained at all the different RCN concentrations, with constant α_e for $RCNH^+$ and $(RCN)_2H^+$ ions and constant k, Figs. 1–4.

The main model used is given in Eq. (5), and plotted in Fig. 2 as a function of [RCN] = [HCN]. This shows that, at an [HCN] = $\sim 1 \times 10^{11}$ cm^{-3}, the α_e of the protonated monomer species can be obtained directly from the slope of the 1/[e^-] vs. time data. This is because [RCN] is too small for any substantial amount of the dimer to form. Conversely, at the highest concentrations used >1×10^{13} cm^{-3}, the proton-bound dimer forms immediately (<0.5 ms) by the association, Eq. (5), and is very much the dominant ion in the plasma after ~1 ms so that from these data the slope is

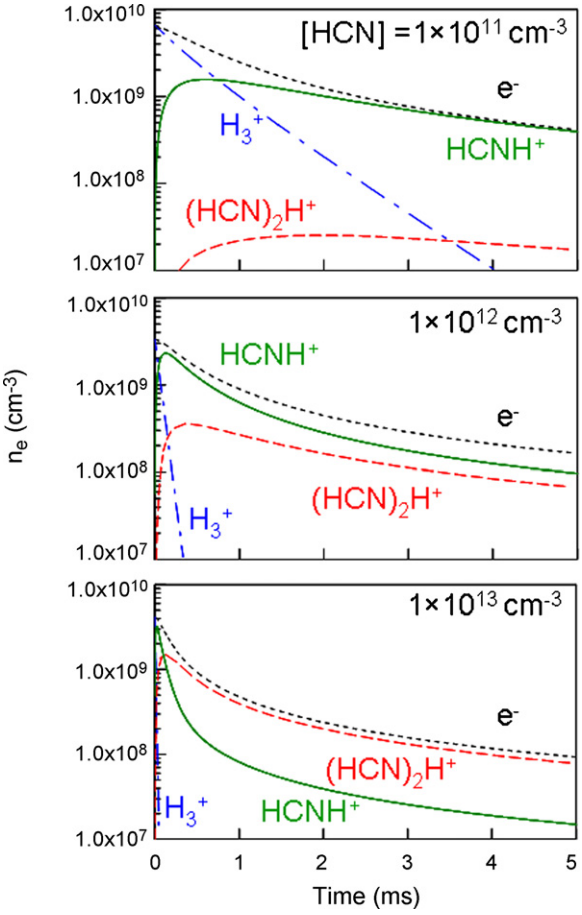

Fig. 2. Electron and ion concentrations in the kinetic model Eq. (5) for HCN are plotted as a function of time in the flow tube. The black dotted lines represent [e⁻], (equals total ion concentration) and the blue dashed-dotted lines are the [H_3^+], which reacts rapidly with HCN for the 1×10^{12} and 1×10^{13} cm^{-3} plots, disappearing in <1 ms. The green solid lines are the $(HCN)H^+$ and the red dashed lines are the $(HCN)_2H^+$. For this illustration, the kinetic model for HCN was arbitrarily chosen, but this behavior is also consistent with the CH_3CN and CH_3CH_2CN studies. (For interpretation of the references to color in this figure legend, the reader is referred to the web version of the article.).

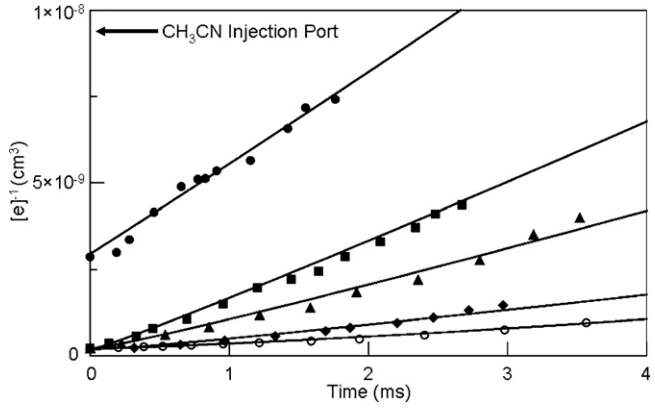

Fig. 3. 1/[e] vs. time plot of the experimental data and fit for [CH_3CN] = (open circles) 1×10^{10} cm^{-3}, (diamonds) 1×10^{11} cm^{-3}, (triangles) 1×10^{12} cm^{-3}, (squares) 1×10^{13} cm^{-3}, and (solid circles) 8×10^{13} cm^{-3}. If only one ionic species is dominant, the α_e is equivalent to the slope. The lines represent the fits for over four orders of magnitude change in [CH_3CN].

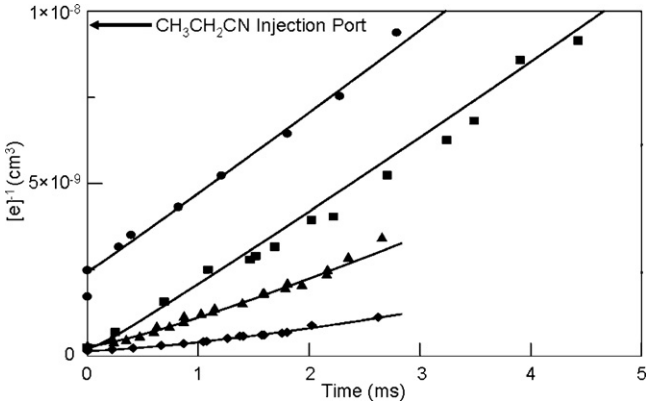

Fig. 4. 1/[e] vs. time plot of the present data and fit (solid lines) for [CH_3CH_2CN] = (diamonds) 1×10^{11} cm^{-3}, (triangles) 1×10^{12} cm^{-3}, (squares) 1×10^{13} cm^{-3}, (circles) 3×10^{13} cm^{-3}. The lines represent the fits for three orders of magnitude change in [CH_3CH_2CN].

equivalent to the α_e of just the proton-bound dimer.

$$\begin{array}{ccccc} & & & \overset{k_5}{} & \\ RCNH^+ + RCN + He & \rightleftharpoons & (RCN)_2H^+ + He & & \\ \downarrow e^- & & \underset{k_{-5}}{} & \downarrow e^- & \end{array} \quad (5)$$

The three-body rate coefficients k_5 for association Eq. (5) to produce these dimers are large. $k_5 = 2.0 \pm 0.5 \times 10^{-26}$ cm^6 s^{-1} is determined from the fits to the model in Eq. (5) for CH_3CN, see Table 1. When considering the effective binary rate coefficient with a [He] = 5.0×10^{16} cm^{-3}, the present value $k_{eff} = k_5$[He] for CH_3CN is only slightly smaller ($k_{eff} = 1.0 \times 10^{-9}$ cm^3 s^{-1}) than with the value previously obtained for CH_3CN ($k_{eff} = 2.1 \times 10^{-9}$ cm^3 s^{-1}) in a flowing afterglow by studying the association reactions in the conventional way [19]. To further improve the model and to obtain a more accurate fit, a two-body reverse reaction rate coefficient of $k_{-5} = 1.0 \pm 2 \times 10^{-13}$ cm^3 s^{-1} for HCN and CH_3CN and $4.0 \pm 3 \times 10^{-14}$ cm^3 s^{-1} for CH_3CH_2CN were also included. This reverse reaction is typical [26,27] for an intermediate complex $[(RCN)_2H^+]^*$ dissociating back into reactants before it can be stabilized by collisions with helium, Eq. (5). A new model, Eq. (6), including the excited intermediate complex was also tried but this only provided the same quality of fit as the Eq. (5) model, but with the addition of an extra recombination rate coefficient for the excited intermediate.

$$\begin{array}{ccccccc} & & \overset{k_6}{} & & \overset{k_{6s}}{} & & \\ RCNH^+ + RCN + He & \rightleftharpoons & [(RCN)_2H^+]^* + He & \rightarrow & (RCN)_2H^+ + He & & \\ \downarrow e^- & & \underset{k_{-6}}{} \downarrow e^- & & & \downarrow e^- & \end{array} \quad (6)$$

However, it is not unreasonable to consider an α_e for the intermediate if the lifetime of the excited complex is relatively long. This possibility is worth noting since the models in Eqs. (5) and (6) require a reverse reaction.

The quality of the fitting to the model is remarkably impressive after assigning the four rate coefficients, see Table 1., because then the only parameter varied in the experiments and in the kinetic model was the concentration of [RCN] and this was varied by approximately four orders of magnitude. A plot of the measured effective DR rate coefficient, α_{eff}, vs. the concentration of [HCN] can be seen in Fig. 5. DR for H_3^+ controls the decay of electron at low concentrations <10^9 cm^{-3}, where the α_e for H_3^+ was measured to be 1.1×10^{-7} cm^3 s^{-1} at 300 K, consistent with previous measurements [28]. The α_{eff} then increases at ~10^9 cm^{-3} to a constant value centered at 3×10^{10} cm^{-3} of 3.5×10^{-7} cm^3 s^{-1} which is the α_e for the $HCNH^+$ ions. Another increase in α_{eff} is observed

Table 1
Ion–molecule rate coefficients (k) and recombination rate coefficients (α_e) which provide the best fit to the electron density decays at all concentrations of RCN. The α_M and α_D represent the values for the protonated monomer and the proton-bound dimer, respectively. Uncertainty for the k's and the α's are ±25% and ±15%, respectively. The $k_{1(Theor.)}$ are the theoretical rate coefficients that were calculated using combined variational transition state theory and classical trajectory theory [29]. NA indicates no data are available.

	HCN	CH_3CN	CH_3CH_2N
$k_{1(Lit.)}$ ($cm^3\ s^{-1}$)	9.5×10^{-9}	9.8×10^{-9}	9.9×10^{-9}
$k_{1(Theor.)}$ ($cm^3\ s^{-1}$)	8.5×10^{-8}	1.1×10^{-8}	1.2×10^{-8}
k_5 ($cm^6\ s^{-1}$)	2.0×10^{-26}	2.0×10^{-26}	2.0×10^{-26}
k_{-5} ($cm^3\ s^{-1}$)	1.5×10^{-13}	2.0×10^{-13}	4.0×10^{-14}
$\alpha_{M(Exp.)}$ ($cm^3\ s^{-1}$)	3.6×10^{-7}	3.4×10^{-7}	4.6×10^{-7}
$\alpha_{M(Lit.)}$ ($cm^3\ s^{-1}$)	FA[29] $3.5 \pm 0.9 \times 10^{-7}$ SR[30] 2.8×10^{-7}	FA[28] $3.3 \pm 1 \times 10^{-7}$ SR[31] $8.1 \pm 0.8 \times 10^{-7}$	FA[28] $4.7 \pm 2 \times 10^{-7}$
$\alpha_{D(Exp.)}$ ($cm^3\ s^{-1}$)	2.4×10^{-6}	2.8×10^{-6}	2.3×10^{-6}
$\alpha_{D(Lit.)}$ ($cm^3\ s^{-1}$)	NA	FA[19] $2.8 \pm 1 \times 10^{-6}$	NA

above $\sim 1 \times 10^{11}$ cm^{-3} until another constant region was observed $>2 \times 10^{12}$ cm^{-3}, where an average α_e for the dimer $(HCN)_2H^+$ ions of 2.4×10^{-6} $cm^3\ s^{-1}$ is obtained. These data show the regions where the concentration of the HCN produced a plasma dominated by either $HCNH^+$ or $(HCN)_2H^+$ and the intermediate values of the α_{eff} due to the transition between these limits. These constant sections also correspond to the same concentration where the kinetic models indicate that just one recombining ion dominates. Fig. 5. indicates very clearly that unless such plots are made and the correct concentrations of the cyanides used, erroneous values of the α_e can very easily be obtained. The concentration dependent plots for CH_3CN and CH_3CH_2CN are similar to that of Fig. 5 for HCN. Without such information it is very dangerous to try to determine α_e for the specific species since any value between that of H_3^+ and the proton-bound dimer can be obtained.

Plot A in Fig. 1, shows the recombination and diffusion of H_3^+ in open circles, which is noticeably slower than the recombination of the $HCNH^+$ and $(HCN)_2H^+$. While the rate of diffusion for H_3^+ is larger than that for the higher mass molecular ions, its α_e is much smaller. Plot A in Fig. 1, has been presented to show the electron density decay at various [HCN]. Note, the electron density decay was monitored over one order of magnitude to ensure that we captured the entire range.

The three-body association and the reverse rate coefficients were varied to determine how much uncertainty would be associated with these values as obtained with the kinetic model, and a standard deviation was calculated for every case. These rate coefficients have an uncertainty of $\lesssim$±25% for all reactions. The three-body association rates for all of the reactions are very similar,

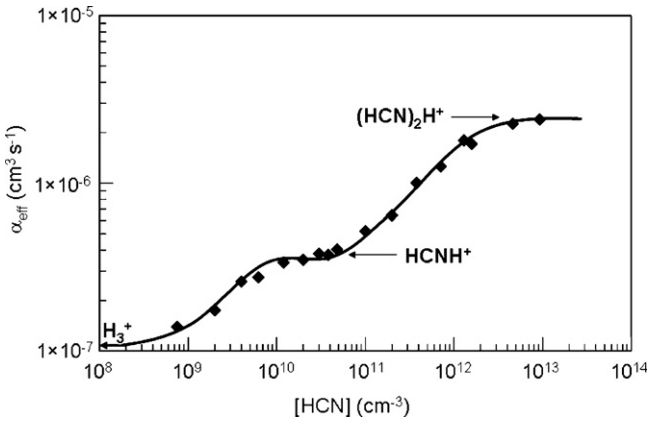

Fig. 5. A plot of α_{eff} vs. [HCN]. The regions where H_3^+, $HCNH^+$ and $(HCN)_2H^+$ control the loss of electrons can be seen from these data and are indicated. The solid line through these data has been included to emphasize the constant α_{eff} regions corresponding to the α_e for $HCNH^+$ and $(HCN)_2H^+$.

but this is not surprising since the dipole moments (d) for these three cyanides are also very similar, with values of 2.98, 3.92, 4.02 Debye for HCN, CH_3CN, and CH_3CH_2CN, respectively [30]. If the forward and reverse ion–molecule reactions are fast compared to electron–ion recombination of $(RCN)_2H^+$ and $RCNH^+$, then an equilibrium can be established, and this has been shown previously to give the appearance of one effective recombination coefficient, α_{eff} [31]. Alternatively, when the forward reaction is fast compared to the reverse, then a dynamic equilibrium can be established due to the rapid recombination rates. In Fig. 1B, 3 and 4, the experimental data for the HCN, CH_3CN and CH_3CH_2CN systems along with the fit (solid lines) shows that the $1/[e^-]$ vs. time plots are consistently close to linear with only very slight deviations due to ambipolar diffusion. The data in these figures are relatively similar showing similar mechanisms. At low [RCN] concentrations, the $[e^-]$ decay is controlled by only the recombination of the monomer and diffusion. As the concentration of RCN increases, the dimer production increases, which begins to contribute more to the total ionization loss, until eventually the dimer is present at a relatively short time after injection $\sim$1 ms and its recombination is followed.

At the highest concentration of RCN, there is a rapid decrease in the electron number density at <1 ms. Such a rapid decrease may be created if the flow tube is being coated with an insulating layer of the reactant vapor, lowering the return area for the probe. Fortunately, as the distance from the injection port increases, a smaller amount of vapor is available to coat the flow tube, and as the electron density decreases the effect on the returned current also decreases. Note that the Langmuir probe had to be cleaned considerably more at these higher concentrations to obtain consistent electron number density measurements. For the CH_3CNH^+ system, the α_e after this initial drop is consistent with previous measurements for the α_e for $(CH_3CN)_2H^+$ at 300 K. To the author's knowledge, this is the only proton-bound dimer in the series to have been measured previously [19]. The magnitudes of the α_e's for $RCNH^+$ compared to the α_e's of $(RCN)_2H^+$ for all three cyanides show that the proton-bound dimers have substantially larger α_e's. In comparing the measured α_e's with the available literature there is a good agreement with previous flowing afterglow measurements where available [12,32]. FA and SR denote previous flowing afterglow and storage ring measurements. The α_e's for $HCNH^+$ using the SR are only slightly smaller than the current measurement and certainly within the combined errors, while the α_e for CD_3CND^+ appears much larger than both of the FA measurements [33]. Note that, the comparison is not exact because CD_3CN was used instead of CH_3CN and the proton transfer reaction was with deuterium instead of hydrogen [34].The α_e's for $HCNH^+$ and CH_3CNH^+ are very similar to the α_e of $CH_3CH_2CNH^+$ which is slightly larger as would be expected for the increasing complexity of the recombining ion. However, when comparing the α_e's for the proton-bound dimers of the three systems, there are important differences. The

α_e for the $(CH_3CN)_2H^+$ is larger than that for the $(HCN)_2H^+$. Interestingly, this trend does not continue for the α_e of $(CH_3CH_2CN)_2H^+$, which is smaller. The smaller α_e for $(CH_3CH_2CN)_2H^+$ may be caused by the larger ethyl chains sterically hindering the electron capture. This implies that the recombination of these proton-bound dimers is very site specific and there is not much variation in α_e with increasing dimer size. This has previously been shown to be the case for proton-bound H_2O clusters and is further evidence that these recombination rates are approaching the upper limit for the dissociative recombination process [35]. In the $(H_2O)_nH^+$, clusters for $n = 2$, 3, 4, 5 the α_e's only varied from (2.5, 3.0, 3.0, 3.6) $\times 10^{-6}$ cm^3 s^{-1}, respectively [18].

4. Conclusions

A comprehensive study has revealed that the recombination of $RCNH^+$ ion is not just a simple recombination situation but that proton-bound dimers begin to contribute more to the electron density decay when the [RCN] is increased above $\sim 10^{11}$ cm^{-3} due to the increasing rate of association. α_e for $RCNH^+$ and $(RCN)_2H^+$ for each of the three systems have been determined and compared to previous data when available, see Table 1. The protonated-cyanides have relatively modest $\alpha_e < 5 \times 10^{-7}$ cm^3 s^{-1} while their proton-bound dimer ions have substantially larger $\alpha_e > 10^{-6}$ cm^3 s^{-1} at 300 K. Note that both individual α_e's can be obtained directly from the slopes of the $1/[e^-]$ vs. time plots without the use of the fitting model if the appropriate concentrations of the cyanides are chosen ([RCN] $\alpha \sim 10^{11}$ cm^{-3} and $\gtrsim 10^{13}$ cm^{-3}, for the $RCNH^+$ and $(RCN)_2H^+$, respectively), see Fig. 2. These specific concentrations can easily be determined by solving the kinetic reaction models as long as the rate coefficients are known for the proton transfer and association reactions. The HCN, CH_3CN and CH_3CH_2CN proton transfer reactions from H_3^+ are extremely rapid $\sim 1 \times 10^{-8}$ cm^3 s^{-1} compared to a typical gas kinetic rate coefficient 2×10^{-9} cm^3 s^{-1} due to their large dipole moments and the small mass of H_3^+. A simple three-body mechanism, Eq. (5) model, was used to fit all of the present data, with a reverse reaction being included to obtain the presented fits. This indicates that at least some of the clusters are excited and can either recombine or dissociate back into the protonated monomer.

Although association of the type presented would be small due to the low concentration of neutral cyanides in the Titan's atmosphere, it has been shown that these type of reactions can compete with moderately rapid DR [36]. However, future studies need to be done to determine the rate of association and subsequent DR of $RCNH^+$ with the dominant neutrals, N_2 and CH_4. It is worthwhile to consider the importance of the present studies to modeling of the Titan atmospheric chemistry. The atmosphere of Titan consists mainly of N_2 (98%) with some methane (2%) and other hydrocarbons with $HCNH^+$ being the dominant ion in the altitude range 1000–1300 km. Chemical modeling [2,3] has shown that $HCNH^+$ is likely formed in the reactions

$$N^+ + CH_4 \rightarrow HCNH^+ + H_2 \quad (7)$$

$$HCN^+ + CH_4 \rightarrow HCNH^+ + CH_3 \quad (8)$$

and lost by

$$HCNH^+ + HC_3N \rightarrow C_3H_2N^+ + HCN \quad (9)$$

and the reversible reaction

$$HCNH^+ + H_2O \rightleftarrows H_3O^+ + HCN \quad (10)$$

An additional loss reaction is the DR

$$HCNH^+ + e \rightarrow \text{neutral products} \quad (11)$$

Further loss can occur by the rapid association

$$HCNH^+ + HCN + N_2 \rightarrow H^+(HCN)_2 + N_2 \quad (12)$$

to produce the rapidly recombining dimer, $H^+(HCN)_2$, although this may not be competitive because of the low concentration of HCN. Alternatively, an association with N_2 or CH_4 can occur

$$HCNH^+ + N_2/CH_4 + N_2 \rightarrow H^+(HCN)\cdot N_2/CH_4 + N_2 \quad (13)$$

followed by recombination or the switching reaction

$$H^+(HCN)\cdot N_2/CH_4 + HCN \rightarrow H^+(HCN)_2 + N_2/CH_4 \quad (14)$$

Similar reaction sequences may also occur for CH_3CNH^+ and $C_2H_5CNH^+$. These three-body reactions (reactions (12) and (13)) will become more important at lower altitudes where there is aerosol formation, [37] below those accessible by the Cassini INMS, but still accessible by radio occultation [38]. Temperature dependent studies also need to be performed to be appropriate for the colder temperatures on Titan [39].

Acknowledgements

Funding under mostly NASA grant no. NAG5-8951 and NSF grant no. 0212398 is gratefully acknowledged.

References

[1] J.L. Fox, R.V. Yelle, Geophys. Res. Lett. 24 (1997) 2179.
[2] C.N. Keller, V. Anicich, T.E. Cravens, Planet. Space Sci. 46 (1998) 1157.
[3] E.H. Wilson, S.K. Atreya, J. Geophys. Res. 109 (2004) E06002.
[4] V. Anicich, P. Wilson, M.J. McEwan, J. Am. Soc. Mass Spectrom. 15 (2004) 1148.
[5] T.E. Cravens, I.P. Robertson, J.H. Waite, R.V. Yelle, W.T. Kasprzak, C.N. Keller, S.A. Ledvina, H.B. Nieman, J.G. Luhmann, R.L. McNutt, W.-H. Ip, V. de la Haye, I. Mueller-Wodarg, J.-E. Wahlund, V.G. Anicich, V. Vuitton, Geophys. Res. Lett. 33 (2006) L07105.
[6] L.M. Ziurys, B.E. Turner, Astron. J. 302 (1986) L31.
[7] L.M. Ziurys, B.E. Turner, Detection of interstellar vibrationally excited HCN, Astron. J. 300 (1986) L19.
[8] B.E. Turner, P. Friberg, W.M. Irvine, M. Saito, S. Yamamoto, Interstellar cyanomethane, Astrophys. J. 355 (2) (1990) 546.
[9] T. Amano, H. Hashimoto, K. Hirao, J. Mol. Struct. 795 (2006) 190.
[10] G.J. Molina-Cuberos, J.J. Lopez-Moreno, R. Rodrigo, L.M. Lara, J.Geophys. Res. 104 (1999) 21997.
[11] G. Bouchoux, T.N. Minh, P. Longevialle, J. Am. Chem. Soc. 114 (1992) 10000.
[12] M. Geoghegan, N.G. Adams, D. Smith, J. Phys. B 24 (1991) 2589.
[13] V. Vuitton, R.V. Yelle, V. Anicich, Astrophys. J. 647 (2006) L175.
[14] G.I. Mackay, D. Betowski, H.I. Payzant, J. Phys. Chem. A 80 (1976) 2919.
[15] D.C. Clary, D. Smith, N.G. Adams, Chem. Phys. Lett. 119 (1985) 320.
[16] V. Anicich, J. Phys. Chem. Ref. Data 22 (6) (1993) 1469.
[17] D.R. Bates, J. Phys. B 24 (1991) 703.
[18] J.B.A. Mitchell, C. Rebrion-Rowe, Int. Rev. Phys. Chem. 16 (1997) 201.
[19] R. Plasil, J. Glosik, P. Zakouril, Formation, J. Phys. B 32 (1999) 3575.
[20] J.L. McLain, V. Poterya, D.M. Jackson, N.G. Adams, L.M. Babcock, J. Phys. Chem. A 109 (2005) 5119.
[21] D. Smith, N.G. Adams, in: W. Lindinger, T.D. Mark, F. Howorka (Eds.), Studies of Plasma Reaction Processes using a Flowing Afterglow/Langmuir Probe Apparatus. In Swarms of Ions and Electrons in Gases, Springer-Verlag, Vienna, 1984, p. 284.
[22] N.G. Adams, D. Smith, in: J.M. Farrar, J.W.H. Saunders (Eds.), Techniques for the Study of Ion–Molecule Reactions, vol. 20, Wiley Interscience, New York, 1988, p. 165.
[23] J.L. McLain, V. Poterya, C.D. Molek, L.M. Babcock, N.G. Adams, J. Phys. Chem. A 108 (2004) 6704.
[24] K. Ziegler, Org. Syn. 7 (1927) 50.
[25] J.D. Swift, M.J.R. Schwar, Electrical Probes for Plasma Diagnostics, Iliffe, London, 1970.
[26] J. Glosik, P. Zakouril, W. Lindinger, Int J. Mass Spectrom. Ion Proc. 145 (3) (1995) 155.
[27] J. Glosik, A. Jordan, V. Skalsky, W. Lindinger, Int J. Mass Spectrom. Ion Proc. 129 (1993) 109.
[28] J. Glosik, R. Plasil, V. Poterya, P. Kudrna, M. Tichy, Chem. Phys. Lett. 331 (2000) 209.
[29] T. Su, W.J. Chesnavich, J. Chem. Phys. 76 (10) (1982) 5183.
[30] R.D. Nelson, Selected Values of Electric Dipole Moments for Molecules in the Gas Phase, *NSRDS-NBS 10* 1971.
[31] O. Novotny, R. Plasil, A. Pysanenko, I. Korolov, J. Glosik, J. Phys. B 39 (2006) 2561.
[32] N.G. Adams, D. Smith, Chem. Phys. Lett. 144 (1988) 11.

[33] J. Semaniak, B.F. Minaev, A.M. Derkatch, F. Hellberg, A. Neau, S. Rosen, R. Thomas, M. Larsson, H. Danared, A. Paal, M. af Ugglas, Astrophys. J. Suppl. 135 (2001) 275.
[34] W.D. Geppert, E. Vigren, M. Hamberg, V. Zhaunerchyk, R.D. Thomas, M. Kaminska, T.J. Millar, J. Semaniak, H. Roberts, F. Hellberg, F. Oesterdahl, A. Ehlerding, M. Larsson, J Phys. Conf. Ser. (2007) 88.
[35] D.R. Bates, J. Phys. B 24 (1991) 3267.
[36] J.H. Waite, H. Nieman, R.V. Yelle, W.T. Kasprzak, T.E. Cravens, J.G. Luhmann, R.L. McNutt, W.-H. Ip, D. Gell, V. de la Haye, I. Muller-Wordag, B. Magee, N. Borggren, S. Ledvina, G. Fletcher, E. Walter, R. Miller, S. Scherer, R. Thorpe, J. Xu, B. Block, K. Arnett, Science 308 (2005) 982.
[37] J.H. Waite, D.T. Young, T.E. Cravens, A.J. Coates, F.J. Crary, B. Magee, J. Westlake, Science 316 (2007) 870.
[38] A.J. Kliore, A.F. Nagy, E.A. Marouf, R.G. French, F.M. Flasar, N.J. Rappaport, A. Anabttawi, S.W. Asmar, D.S. Kahann, E. Barbinis, G.L. Goltz, D.U. Fleischman, D.J. Rochblatt, J. Geophys. Res. 113 (2008) A09317.
[39] J.L. McLain, N.G. Adams, Flowing afterglow studies of temperature dependencies for electron recombination of $HCNH^+$, CH_3CNH^+ and $CH_3CH_2CNH^+$ and their proton bound dimers. Planet. Space Sci., submitted.